



**HAL**  
open science

## Diversification of tiny toads (Bufonidae: Amazophrynella ) sheds light on ancient landscape dynamism in Amazonia

Leandro Moraes, Fernanda Werneck, Alexandre Réjaud, Miguel Rodrigues, Ivan Prates, Frank Glaw, Philippe Kok, Santiago Ron, Juan Chaparro, Mariela Osorno-Muñoz, et al.

### ► To cite this version:

Leandro Moraes, Fernanda Werneck, Alexandre Réjaud, Miguel Rodrigues, Ivan Prates, et al.. Diversification of tiny toads (Bufonidae: Amazophrynella ) sheds light on ancient landscape dynamism in Amazonia. *Biological Journal of the Linnean Society*, 2022, 136 (1), pp.75-91. 10.1093/biolinnean/blac006 . hal-03869388

**HAL Id: hal-03869388**

**<https://hal.science/hal-03869388>**

Submitted on 24 Nov 2022

**HAL** is a multi-disciplinary open access archive for the deposit and dissemination of scientific research documents, whether they are published or not. The documents may come from teaching and research institutions in France or abroad, or from public or private research centers.

L'archive ouverte pluridisciplinaire **HAL**, est destinée au dépôt et à la diffusion de documents scientifiques de niveau recherche, publiés ou non, émanant des établissements d'enseignement et de recherche français ou étrangers, des laboratoires publics ou privés.

1 **Diversification of tiny toads (*Bufonidae: Amazophrynella*) sheds light on**  
2 **ancient landscape dynamism in Amazonia**

3

4 LEANDRO J.C.L. MORAES<sup>1,2,\*</sup>, FERNANDA P. WERNECK<sup>2</sup>, ALEXANDRE  
5 RÉJAUD<sup>3</sup>, MIGUEL T. RODRIGUES<sup>1</sup>, IVAN PRATES<sup>4</sup>, FRANK GLAW<sup>5</sup>, PHILIPPE  
6 J.R. KOK<sup>6,7</sup>, SANTIAGO R. RON<sup>8</sup>, JUAN C. CHAPARRO<sup>9</sup>, MARIELA OSORNO-  
7 MUÑOZ<sup>10</sup>, FRANCISCO DAL VECHIO<sup>1</sup>, RENATO S. RECODER<sup>1</sup>, SÉRGIO  
8 MARQUES-SOUZA<sup>1</sup>, ROMMEL R. ROJAS<sup>11</sup>, LÉA DEMAY<sup>3</sup>, TOMAS HRBEK<sup>12</sup>,  
9 ANTOINE FOUQUET<sup>3</sup>

10

11 <sup>1</sup> *Universidade de São Paulo, Instituto de Biociências, Departamento de Zoologia, São*  
12 *Paulo, SP, Brazil*

13 <sup>2</sup> *Instituto Nacional de Pesquisas da Amazônia (INPA), Coordenação de Biodiversidade,*  
14 *Av. André Araújo 2936, 69067-375, Manaus, AM, Brazil*

15 <sup>3</sup> *Laboratoire Evolution et Diversité Biologique, UMR 5174, CNRS, IRD, Université Paul*  
16 *Sabatier, Bâtiment 4R1 31062 cedex 9, 118 Route de Narbonne, 31077 Toulouse, France*

17 <sup>4</sup> *Department of Ecology and Evolutionary Biology and Museum of Zoology, University of*  
18 *Michigan, Ann Arbor, MI, USA*

19 <sup>5</sup> *Zoologische Staatssammlung München (ZSM-SNSB), Münchhausenstr. 21, 81247*  
20 *München, Germany*

21 <sup>6</sup> *Department of Ecology and Vertebrate Zoology, Faculty of Biology and Environmental*  
22 *Protection, University of Łódź, 12/16 Banacha Str., Łódź 90-237, Poland*

23 <sup>7</sup> *Department of Life Sciences, The Natural History Museum, London SW7 5BD, United*  
24 *Kingdom*

25 <sup>8</sup> *Museo de Zoología, Facultad de Ciencias Exactas y Naturales, Pontificia Universidad*  
26 *Católica del Ecuador, Quito, Ecuador*

27 <sup>9</sup> *Museo de Biodiversidad del Perú, Urbanización Mariscal Gamarra A-61, Zona 2, Cusco,*  
28 *Peru*

29 <sup>10</sup> *Instituto Amazónico de Investigaciones Científicas SINCHI. Sede enlace. Calle 20 # 5-*  
30 *44, Bogotá, Colombia*

31 <sup>11</sup> *Facultad de Ciencias Biológicas, Departamento de Ecología y Fauna, Universidad*  
32 *Nacional de la Amazonía Peruana-UNAP, Av. Grau 1072, Iquitos, Peru*

33 <sup>12</sup> *Universidade Federal do Amazonas, Instituto de Ciências Biológicas, Av. General*  
34 *Rodrigo Octávio Jordão Ramos, 1200, 69080-900, Manaus, AM, Brazil*

35

36 \* Corresponding author. E-mail: leandro.jclm@gmail.com

37

38 **Running head:** Diversification of *Amazophrynella*

39

40 **Author contributions:** A.F, L.J.C.L.M. and F.P.W. conceived the study. A.F., M.T.R.,  
41 S.R., J.C.C., F.G., P.J.R.K., M.O.M., R.R.R., T.H., F.D.V., R.S.R. and S.M.S. conducted  
42 sampling. A.F., A.R. and L.D. generated DNA sequence data. L.J.C.L.M., A.R. and A.F.  
43 analysed the data; L.J.C.L.M. and A.F. led the writing; and all authors reviewed the final  
44 draft.

45 **ABSTRACT.** Major historical landscape changes have left significant signatures on  
46 species diversification. However, how these changes have affected the build-up and  
47 maintenance of Amazonia's megadiversity is still debated. Here, we addressed this issue by  
48 focusing on the evolutionary history of a pan-Amazonian toad genus that has diversified  
49 throughout the Neogene (*Amazophrynella*). Based on a comprehensive spatial and  
50 taxonomic sampling (X samples, all nominal species), we delimited Operational  
51 Taxonomic Units from mtDNA sequences. We delimited 35 OTUs among which 13  
52 correspond to nominal species, suggesting a vast underestimation of species richness. Next,  
53 we inferred time-calibrated phylogenetic relationships among OTUs based on complete  
54 mitogenomic data, which confirmed an ancient divergence between two major clades  
55 distributed in eastern and western Amazonia respectively. Ancestral area reconstruction  
56 analyses suggest that the Andean foothills and the Brazilian Shield region represent the  
57 ancient core areas for their diversification. These two clades were likely isolated from each  
58 other by lacustrine ecosystems in western Amazonia during the Miocene, and display a  
59 pattern of northward and eastward dispersals throughout the Miocene–Pliocene. Given the  
60 ecological association of *Amazophrynella* with non-flooded forests, our results reinforces  
61 the perception that ancient Amazonian landscape changes had a major impact on the  
62 diversification of terrestrial vertebrates.

63

64 **ADDITIONAL KEYWORDS:** Amphibia – biogeography – mitogenomics – Neotropics –  
65 Pebas system – *terra firme*

## 66 INTRODUCTION

67 Amazonia has experienced dramatic geomorphologic and climatic changes leading to major  
68 landscape changes over the Cenozoic (Hoorn *et al.*, 2010; Albert *et al.*, 2018). Those  
69 changes have been invoked to explain this region's high species richness and current  
70 biological distributional patterns (Antonelli & Sanmartín, 2011; Leite & Rogers, 2013;  
71 Bicudo *et al.*, 2019). However, despite major improvements in our comprehension of these  
72 landscape changes (Hoorn *et al.*, 2010; Antonelli *et al.*, 2018), the timing of these changes  
73 and how they have affected the diversification of organisms remain unclear. For example,  
74 most studies investigating diversification processes within Amazonia focused on birds,  
75 which mostly diversified over a relatively recent timeframe (< 5 Ma) within this region  
76 (Silva *et al.*, 2019). Other studies have focused on current patterns of community  
77 composition in vertebrate groups but did not investigate historical processes (Oliveira *et al.*,  
78 2017; Godinho & da Silva, 2018; Vacher *et al.*, 2020). One of the reasons for the scarcity  
79 of biogeographic studies in other animal groups comes from challenges of obtaining a  
80 comprehensive spatial sampling due to the difficulty to access many Amazonian regions  
81 (Vacher *et al.*, 2020). In fact, the few biogeographic studies investigating the diversification  
82 of small terrestrial Amazonian vertebrates such as amphibians and squamates, which  
83 supposedly disperse less efficiently than birds and large mammals, generally unraveled  
84 much older events on comparable spatial scales, which may suggest a role of ancient  
85 historical landscape changes in their diversification (Fouquet *et al.*, 2012a, b, 2014; Kok *et*  
86 *al.*, 2017, 2018; Marques-Souza *et al.*, 2020; Moraes *et al.*, 2020; Réjaud *et al.*, 2020).

87         During the Neogene (ca. 23–2.5 million years ago–Myr), Amazonia experienced  
88 intense geomorphological dynamism related to Andean orogeny in the western portion of  
89 the South American plate (Albert *et al.*, 2018; Bicudo *et al.*, 2019). The uplift of this

90 mountain range notably led to the closing of an estuary at the western end of a  
91 hydrographic system running towards the Pacific Ocean some 23 Myr (Hoorn *et al.*, 2010;  
92 Bicudo *et al.*, 2019). Consequently, western Amazonia has probably been covered by an  
93 enormous lacustrine ecosystem that drained into the Caribbean sea to the north (the current  
94 Orinoco drainage) until ca. 9 Myr (the “Pebas System”; Wesselingh & Salo, 2006; Hoorn *et*  
95 *al.*, 2010, 2017). Recent evidence completed the picture by proposing a watershed in  
96 western Amazonia segregating a deep aquatic system along the Andes from a central  
97 fluviotidal basin covered by extensive seasonally flooded habitats to the east (Bicudo *et al.*,  
98 2019). About 9 Myr, the orogeny of the northern Andes and continuous sedimentation of  
99 these aquatic systems, mainly with the young Andean sediments, have ultimately led to a  
100 shift of the flow of this proto-Amazon River system toward the Atlantic Ocean (Hoorn *et*  
101 *al.*, 2010). A biologically diverse mega-wetland (the “Acre System”; Latrubesse *et al.*,  
102 2010) has apparently persisted in southwestern Amazonia for ca. 3 million years after the  
103 establishment of this eastward flow. Subsequent late Miocene erosion favored the  
104 progressive development of non-flooded (*terra firme*) forests and frequent hydrological  
105 changes in this region, ultimately leading to the modern configuration of the Amazon River  
106 and its tributaries (Albert *et al.*, 2018). It is noteworthy that the timeframe and the  
107 amplitude of these changes are still discussed (Hoorn *et al.*, 2010, 2017; Latrubesse *et al.*,  
108 2010) and their consequences on biotic diversification remain elusive.

109         Anuran amphibians often display distinct biogeographic patterns as compared to  
110 other vertebrate taxa because they have finely tuned environmental preferences and  
111 functional characteristics often associated with limited dispersal ability (Moraes *et al.*,  
112 2016; Wollenberg-Valero *et al.*, 2019). These characteristics make their populations  
113 particularly sensitive to the aforementioned historical events, which ultimately lead to

114 striking spatial and temporal signatures in their distributional patterns and phylogenetic  
115 relationships (Fouquet *et al.*, 2012a, 2014). The tiny toads of the pan-Amazonian genus  
116 *Amazophrynella* Fouquet *et al.*, 2012a,b perfectly falls into this description since they all  
117 are similarly small-bodied, mostly associated with the leaf-litter of *terra firme* forests, and  
118 breed in small temporary ponds (Fouquet *et al.*, 2012a; Rojas *et al.*, 2018). The entire genus  
119 appears to display highly conserved ecology, morphology and habitat use (Rojas *et al.*,  
120 2018). Its external morphology is so conserved that until the 1990s, only one described  
121 species was supposed to occupy the entire Amazonia. However, the taxonomic knowledge  
122 has increased rapidly in recent years, with the description of eleven new species over the  
123 past decade (e.g., Rojas *et al.*, 2018; Kaefer *et al.*, 2019; Mângia *et al.*, 2020). Thirteen taxa  
124 are currently recognized, which led to the realization that all species of *Amazophrynella*  
125 have in fact small and almost completely allopatric ranges (Rojas *et al.*, 2018).  
126 Furthermore, phylogenetic analyses based on molecular data suggest that the genus started  
127 to diversify as early as 25 Myr with an initial divergence between two major clades largely  
128 restricted to geomorphologically and climatically distinct western and eastern Amazonian  
129 regions (Fouquet *et al.*, 2012a; Rojas *et al.*, 2018). Subsequent divergences between  
130 northern vs. southern lineages in each of these major clades suggest a role of the  
131 transcontinental Amazon River as a geographical barrier (Rojas *et al.*, 2018). However,  
132 some knowledge gaps persist regarding the actual species richness and phylogenetic  
133 relationships within *Amazophrynella*, as numerous recently identified mitochondrial DNA  
134 (mtDNA) lineages (Vacher *et al.*, 2020) were not yet included in a phylogenetic  
135 reconstruction of the whole genus. In addition, many undersampled areas in Amazonia  
136 probably harbor additional species (Fouquet *et al.*, 2012a; Rojas *et al.*, 2018).

137           Given the ancient origin of *Amazophrynella*, its striking ecological conservatism,  
138 and the dynamic landscape of the Amazonia during Neogene, we hypothesize that major  
139 geomorphological changes have fragmented and imposed barriers to dispersal for these  
140 toads. More specifically, given the early split between a western and an eastern clades  
141 within the genus (Rojas *et al.*, 2018), we hypothesize that the development of broad  
142 lacustrine ecosystems across western Amazonia has isolated the ancestors of these two  
143 major clades along the Andean foothills to the west and the crystalline shields (Guiana and  
144 Brazilian shields) to the east, respectively, where they diversified in isolation until ca. 9  
145 Myr. We also hypothesize that the diversification of the western clade after the demise of  
146 these lacustrine systems (9 Myr onwards) was linked to the progressive expansion of *terra*  
147 *firme* forests and a dynamic riverine system (Hoorn *et al.*, 2010; Pupim *et al.*, 2019).  
148 Conversely, we hypothesize that the diversification of the eastern clade, notably the  
149 divergence between species from the Guiana Shield to the north and Brazilian Shield to the  
150 south, either predates or is concomitant with the establishment of the transcontinental  
151 Amazon River (Hoorn *et al.*, 2010). To test these hypotheses, we gathered an  
152 unprecedented spatial sampling throughout Amazonia (286 sequences of the 16S gene),  
153 including all of the extant species of *Amazophrynella* plus sequences from newly sampled  
154 regions, and reevaluated their boundaries. We then gathered mitogenomic data for most of  
155 the delimited species to investigate phylogenetic relationships and historical biogeography  
156 within the genus based on ancestral area reconstruction and diversification analyses.



## 157 MATERIAL AND METHODS

### 158 INPUT DATA CONSTRUCTION

159 We focused on the 16S mitochondrial gene for the species delimitation analyses, because  
160 this gene has been widely used in studies targeting *Amazophrynella* (e.g., Rojas *et al.*,  
161 2018) and is recognized as one of the universal barcodes for Neotropical amphibians  
162 (Vences *et al.*, 2005b). We gathered geolocalized 16S sequences from 286 specimens (69  
163 newly acquired and 217 that were previously deposited in GenBank) covering almost the  
164 entire distributional range of the genus (Supporting Information, Fig. S1). Details of the  
165 16S sequencing process for newly generated data are presented in the Supporting  
166 Information, Appendix A. Regarding previously published data, we found missing blocks  
167 and several instances of incongruences among voucher numbers, accession numbers,  
168 species labels, and geographic coordinates for GenBank sequences (mostly from Rojas *et*  
169 *al.*, 2018). Therefore, we excluded most of these sequences, keeping only the unambiguous  
170 ones and those representing taxa not sampled by us (Supporting Information, Table S1). A  
171 summary (most likely conservative) of these incongruences is presented in Supporting  
172 Information, Table S2.

173 We selected a representative terminal for most of the delimited OTUs to build a  
174 mitogenomic dataset and reconstruct a time-calibrated phylogenetic hypothesis. Complete  
175 mitogenomes were obtained through low-coverage shotgun sequencing for X OTUs. Due to  
176 the low coverage in some regions, two of the OTUs were represented by only 13–14 loci  
177 from the complete mitogenome (15 loci). For the remaining 13 *Amazophrynella* OTUs for  
178 which complete mitogenomes were not available, we gathered all available mitochondrial  
179 loci (12S, 16S, COI) from GenBank with unambiguous metadata (Supporting Information,  
180 Appendix B). We also incorporated the same outgroups used in the species delimitation

181 analyses. Complete mitogenomes were already available for nine outgroup bufonid genera  
182 in GenBank (*Anaxyrus*, *Bufo*, *Bufo*, *Duttaphrynus*, *Epidalea*, *Leptophryne*,  
183 *Parapelophryne*, *Rhinella* and *Strauchbufo*), and we generated novel complete mitogenome  
184 data for seven genera (*Atelopus*, *Dendrophryniscus*, *Frostius*, *Melanophryniscus*,  
185 *Oreophrynella*, *Osornophryne* and *Rhaebo*). Lastly, to complete the mitogenomic matrix  
186 for the outgroups, we retrieved all available mitochondrial loci (12S, 16S, COI, ND1, ND2  
187 and Cytb) for the remaining four bufonid genera (*Incilius*, *Nannophryne*, *Pedostibes* and  
188 *Peltophryne*) (Supporting Information, Table S1). After discarding the d-loop region and  
189 tRNAs from mitogenomes, we extracted the rDNA (12S, 16S) and protein-coding genes  
190 (ND1, ND2, COI, COII, ATP6, COIII, ND3, ND4L, ND4, ND5, ND6, Cytb). Additional  
191 details of the mitogenome sequencing, assembling and annotation are available in the  
192 Supporting Information, Appendix B.

193

#### 194 SPECIES DELIMITATION

195 Aiming to circumvent potential ambiguities on current species boundaries in  
196 *Amazoprhyne*, we relied on a molecular delimitation of Operational Taxonomic Units  
197 (OTUs). We acknowledge that integrative taxonomy, i.e., the integration of multiple lines  
198 of evidence such as morphological and acoustic data along with DNA, would be preferable  
199 to delimit species (Padial *et al.*, 2010). However, those data are largely missing, and  
200 molecular data can provide a yet approximative but effective overview of the species  
201 diversity existing in a focal clade (Vences *et al.*, 2005a; Fouquet *et al.*, 2007; Paz &  
202 Crawford, 2012).

203 We aligned the 16S sequences on the MAFFT online server with default parameters  
204 except by the use of the E-INS-i strategy, which is indicated for data with multiple

205 conserved domains and long gaps (Katoh & Standley, 2013). The resulting alignment was  
206 used to delimit *Amazophrynella* OTUs based on the combined analysis of three molecular-  
207 based species delimitation methods, each with distinct advantages and limitations in  
208 recognizing evolutionary lineages (Ratnasingham & Hebert 2013; Luo *et al.*, 2017). These  
209 methods included the distance-based Assemble Species by Automatic Partitioning (ASAP;  
210 Puillandre *et al.*, 2021), and two tree-based methods, the multi-rate Poisson Tree Processes  
211 model (mPTP; Kapli *et al.*, 2017), and the Generalized Mixed Yule Coalescent approach  
212 (GMYC; Fujisawa & Barraclough, 2013).

213         The ASAP delimitation was performed on the online server  
214 (<https://bioinfo.mnhn.fr/abi/public/asap/asapweb.html>) considering a simple distance model  
215 to compute the distances between samples, and default parameters. We kept the  
216 delimitation scheme supported by the lowest ASAP score (Puillandre *et al.*, 2021). For the  
217 mPTP delimitation, we first reconstructed a maximum likelihood (ML) phylogenetic tree  
218 with RAxML 8.2.4 (Stamatakis, 2014), running 1,000 nonparametric bootstrap replicates to  
219 assess nodal support. The best-fitted model for our dataset was GTR+G+I according to the  
220 Bayesian Information Criterion (BIC; Hurvich & Tsai, 1989) in a PARTITIONFINDER 2.1.1  
221 (Lanfear *et al.*, 2017) analysis. However, for the ML inference, we did not consider the  
222 estimation of Invariable Sites proportion (*I* parameter) as it prevents reliable estimates of  
223 the other parameters (Stamatakis, 2014). We rooted the tree with 18 outgroups, including  
224 12 of the 14 New-World genera of Bufonidae (*Atelopus*, *Dendrophryniscus*, *Frostius*,  
225 *Melanophryniscus*, *Rhinella*, *Anaxyrus*, *Incilius*, *Nannophryne*, *Oreophrynella*,  
226 *Osornophryne*, *Peltophryne* and *Rhaebo*) and eight Old-World genera (*Bufo*, *Bufotes*,  
227 *Duttaphrynus*, *Epidalea*, *Leptophryne*, *Parapelophryne*, *Strauchbufo* and *Pedostibes*)  
228 (Supporting Information, Table S1). This sampling accounts for all genera with available

229 molecular data from the paraphyletic group of “atelopodids” (i.e. taxa branching near the  
230 base of the Bufonidae tree; Kok *et al.*, 2018). Using the resulting ML tree, we ran the  
231 mPTP delimitation on the EDB-calc cluster (Toulouse, France), with 50 million Markov  
232 chain Monte Carlo (MCMC) iterations, sampling every 100,000 iterations and discarding  
233 10% of initial burn-in.

234         For the GMYC delimitation, we obtained an ultrametric phylogeny by  
235 reconstructing a time-calibrated Bayesian tree using the software BEAST 2.6.3 (Bouckaert *et*  
236 *al.*, 2014) with the GTR+G+I substitution model, and using only unique haplotypes. We  
237 used a birth-death process to model speciation and extinction (Gernhard, 2008), and an  
238 uncorrelated relaxed clock to model evolutionary rate variation among branches  
239 (Drummond *et al.*, 2006). In the absence of fossil records for *Amazophrynella* and closely  
240 related genera, we calibrated the tree using two secondary node constraints based on time-  
241 calibrated anuran phylogenies inferred from comprehensive genomic datasets and fossil  
242 calibrations (Feng *et al.*, 2017; Hime *et al.*, 2021). These dates were constrained with a  
243 normal prior distribution and included: (1) the crown age of Bufonidae (Mean = 48.0 Myr,  
244 SD = 2.5), and (2) the divergence time of *Amazophrynella* + *Dendrophryniscus* vs.  
245 remaining bufonids (Mean = 35.4 Myr, SD = 2.4). MCMC parameters were set to four  
246 parallel runs with 100 million iterations, 10,000 of thinning and 10% of initial burn-in. We  
247 checked the convergence of parameters (ESS > 200) of the combined log file of four runs  
248 with TRACER 1.7 (Bouckaert *et al.*, 2014; Rambaut *et al.*, 2018) and extracted the  
249 maximum clade credibility tree using TREE ANNOTATOR 2.6.3 (Bouckaert *et al.*, 2014). We  
250 performed the multiple threshold GMYC delimitation using only the *Amazophrynella* clade  
251 of this ultrametric tree using the GMYC function of the ‘splits’ R package (Ezard *et al.*,  
252 2014) with a threshold interval between 0–10 Myr.

253 We defined the distinct Operational Taxonomic Units (OTUs) based on the  
254 combined evidence of these three delimitation methods (i.e., congruence between the  
255 results of at least two of them), and the stability of the current taxonomic knowledge of the  
256 genus (i.e., by considering each of the currently valid species as distinct OTUs). Some of  
257 these OTUs included specimens from the type series of nominal species; others specimens  
258 could be attributed to nominal taxa because the range of corresponding OTUs spanned the  
259 type localities of these taxa (see Supporting Information, Appendix C). Lastly, with MEGA  
260 7 (Kumar *et al.*, 2016), we estimated the mean uncorrected genetic distances (p-distances)  
261 among OTUs.

262

### 263 **TIME-CALIBRATED PHYLOGENETIC RELATIONSHIPS**

264 We aligned each locus of the mitogenomes independently using the MAFFT online server  
265 with default parameters, except for the use of E-INS-i strategy for rDNA, with multiple  
266 conserved domain and long gaps, and the G-INS-i strategy for CDS, which is  
267 recommended for sequences with global homology (Kato & Standley, 2013). Coding  
268 regions were realigned considering reading frame, and individual alignments were  
269 concatenated using GENEIOUS 9.1.8 (Kearse *et al.*, 2012). We estimated the best-fitting  
270 partition scheme and model of evolution for each partition comparing the BIC in a  
271 PARTITIONFINDER analysis. Our predefined division of this dataset considered a single  
272 partition for rDNA and one for each codon position of the protein coding genes (CDS1,  
273 CDS2, CDS3). Best-fitted substitution models were GTR+I+G for rDNA, CDS1 and  
274 CDS2, and TNR+I+G for CDS3. Using the final alignment, resulting partition schemes and  
275 best-fitted substitution models, we reconstructed a time-calibrated Bayesian phylogenetic  
276 tree with BEAST. Parameters of the analysis, MCMC runs, and ages for node calibrations

277 were identical to those described in GMYC species delimitation analysis. We are aware that  
278 incorporating mtDNA only in our phylogenetic analyses may lead to overestimation of  
279 divergence times (McCormack *et al.*, 2011). However, given the challenges to sample  
280 Amazonian organisms comprehensively, we focus on obtaining greater taxonomic and  
281 geographical breadth rather than genomic coverage. Our resulting hypotheses can be  
282 explicitly tested with the accumulation of knowledge from the integration of future nuDNA  
283 information.

284

#### 285 **BIOGEOGRAPHIC ANALYSES**

286 The time-calibrated mitogenomic tree obtained from the BEAST analysis was used to  
287 perform an ancestral area reconstruction using the ‘BioGeoBEARS’ R package (Matzke,  
288 2013), which infers the geographic distribution of ancestral species and speciation events.  
289 As this package requires an attribution of species distributions as proxies of biogeographic  
290 regions, we performed two analyses considering different partitioning schemes of  
291 Amazonia. Under the combined evidence of these two approaches, we aim at identifying  
292 broad and refined geographic patterns of the group diversification, allowing the testing of  
293 hypotheses related to ancient and more recent Amazonian landscape changes. First, we  
294 considered a broad delimitation of biogeographic regions based on the Wallacean districts  
295 (Wallace, 1854), defined as wide units following main geological compartments and  
296 landscape features of this region: 1) western Amazonia (WA), corresponding to the  
297 sedimentary Solimões basin, and 2) Guiana Shield (GS) and 3) Brazilian Shield (BS),  
298 corresponding to the crystalline shields. These units were delimited by the large rivers  
299 Negro, Madeira and the lower course of the Amazon, known to correspond to major breaks  
300 in amphibian community composition across Amazonia (Godinho & da Silva, 2018;

301 Vacher *et al.*, 2020). The second partitioning considered a refined delimitation based on  
302 “Areas of Endemism”, historically defined in Amazonian biogeographic studies of birds  
303 and primates (Cracraft, 1985). These areas are mostly limited by the large rivers of the  
304 region, as follows (riverine boundaries in parenthesis): Inambari (IN; Huallaga–Madeira),  
305 Napo (NA; Japurá–Amazon), Imeri (IM; Japurá–Negro), Guiana (GU; Negro–Amazon,  
306 corresponding to the Guiana Shield), Rondonia (RO; Madeira–Tapajós), Tapajós (TA;  
307 Tapajós–Xingu) and Xingu (XI; Xingu–Tocantins). Members of *Amazophrynella* are not  
308 known to occur in other classic Areas of Endemism, such as Belem (eastwards Tocantins  
309 River), at high elevations in the Pantepui region, or [from the easternmost Solimões–Negro](#)  
310 [interfluve \(Jaú Area of Endemism\) \(Borges & Silva, 2012\)](#) (Supporting Information, Fig.  
311 S1). These areas of [endemism were thus not included in our analyses](#). Considering that  
312 OTUs within *Amazophrynella* were spatially restricted, mostly occurring within single  
313 areas, we set the maximum number of ancestral areas to two for the broad-partitioning  
314 analysis and three for the refined one, and excluded non-adjacent ancestral distributions to  
315 narrow down ancestral states.

316 In ‘BioGeoBEARS’, three diversification models with distinct premises were  
317 compared: Dispersal Extinction Cladogenesis (DEC; Ree & Smith, 2008), Dispersal-  
318 Vicariance (DIVALIKE; Ronquist, 1997), and BayArea (BAYAREA; Landis *et al.*, 2013).  
319 We also considered those three models including founder-event speciation (J parameter;  
320 Matzke, 2013), but because the utility of this parameter has been debated (Ree &  
321 Sanmartin, 2018; Klaus & Matzke, 2020), we discussed the differences between the results  
322 of best-fitted models considering or not this parameter. Model fit was assessed under the  
323 Akaike Information Criterion (AIC). To further investigate the frequency and geographic  
324 context of biogeographic events (i.e., vicariance, dispersal, and sympatric speciation), we

325 conducted a Biogeographical Stochastic Mapping (BSM) analysis implemented in  
326 ‘BioGeoBEARS’ (Dupin *et al.*, 2017). With BSM, we simulated 50 possible biogeographic  
327 scenarios accounting for the same pattern of diversification as the best-fit model to obtain  
328 an estimate of event frequencies across simulations (mean  $\pm$  standard deviation). To  
329 perform this analysis, we used the same dataset and distinct schemes of spatial partitioning  
330 (broad and refined) used in the ancestral area reconstruction analysis.

331 Finally, we tested if and when the diversification rate of *Amazophrynella* varied  
332 through time using Lineage Through Time (LTT) analyses. We conducted a Monte Carlo  
333 Constant Rate (MCCR) analysis using the ‘LASER’ 2.4.1 R package (Pybus & Harvey,  
334 2000; Rabosky, 2006) to test if the observed diversification pattern is significantly different  
335 from the expected from a Yule pure-birth model while accounting for randomly distributed  
336 missing taxa. Using the same package, we compared the fit of seven models of  
337 diversification: two constant-rate Yule models (pure-birth and birth-death), two density-  
338 dependent models (DDX and DDL), and the Yule-n-rate model accounting for two, three  
339 and four changes in speciation rates across the tree. We determined the best-fit model by  
340 comparing AIC values. Using the ‘ape’ 5.3 R package (Paradis *et al.*, 2004), we plotted the  
341 empirical lineage accumulation through time relative to that expected under a Yule pure-  
342 birth model with a 95% confidence interval.

343

#### 344 **DATA AVAILABILITY**

345 Newly generated DNA sequences will be submitted to GenBank upon acceptance of this  
346 study (Supporting Information, Table S1). R scripts used for the phylogenetic  
347 reconstruction and the biogeographic inferences were the same from Réjaud *et al.* (2020).



348 Additional data underlying this study are available in the Supporting Information, or  
349 directly from the corresponding author upon request.

## 350 RESULTS

### 351 SPECIES DELIMITATION

352 The resulting 16S alignment consisted of 491 nucleotide sites. The partitioning from the  
353 three species delimitation methods (ASAP, mPTP and GMYC) display rare hard  
354 incongruences but extensive difference in their subdivisions. The mPTP method was the  
355 most conservative, recovering 15 OTUs, whereas the ASAP and the GMYC methods  
356 recovered 39 and 40 OTUs, respectively (Supporting Information, Fig. S2). The mPTP  
357 method can be considered overconservative, since nine nominal species were lumped  
358 within three OTUs. By contrast, in a few instances the ASAP and GMYC methods split  
359 geographically adjacent populations and even samples from the type series of a single  
360 nominal species (*A. matses*) into distinct OTUs (Supporting Information, Fig. S2). We  
361 therefore attempted to maximize the consensus across these three methods while  
362 minimizing seemingly spurious splits by considering the current taxonomic knowledge of  
363 the genus and distributions of taxa. Delimitation of OTUs was notably conflictual across  
364 methods for the subclade formed by *A. minuta*, *A. siona* and *A. amazonicola* (see below)  
365 (Supporting Information, Fig. S2). We delimited those three nominal species as distinct  
366 OTUs given their segregation in geographic space and morphological distinctiveness (Rojas  
367 *et al.*, 2018). Our delimitation approach resulted in 35 OTUs (Fig. 1) distributed equally  
368 across the two major clades, with 18 (western) and 17 (eastern) OTUs (Fig. 1A). With 13  
369 nominal species currently recognized in the genus, this delimitation corresponds to almost a  
370 threefold increase in richness.

371 The minimum mean genetic distance between OTUs according to this delimitation  
372 is 2.7 % (corresponding to the comparison between *A. vote* and *A. OTU10*). Intraspecific  
373 distances only slightly surpassed this minimum threshold in the case of *A. OTU2* (3.1 %),

374 but were mostly below 2.1 % (Supporting Information, Table S3). Geographic distributions  
375 of the delimited OTUs revealed a striking allopatric pattern, with very limited overlap  
376 among closely related OTUs. Cases of spatial overlap among related OTUs seem more  
377 common in eastern Amazonia (a region better represented in our sampling), but most OTUs  
378 were found to be micro-endemic or narrowly distributed (Fig. 1B). *Amazophrynella siona*  
379 and *A. minuta* from northwestern Amazonia, and *A. manaos* and *A. teko* from the Guiana  
380 Shield region, display the widest ranges (Fig. 1B).

381

## 382 **PHYLOGENETIC RELATIONSHIPS AND TEMPO OF CLADOGENESIS**

383 The mitogenomic phylogeny was based on an alignment of 13,888 nucleotide sites and 55  
384 terminals. This phylogenetic inference yielded a strongly supported topology with the  
385 majority of nodes showing posterior probabilities support  $> 0.95$  (Fig. 2).  
386 *Melanophryniscus* was inferred as the sister of all other bufonid genera, followed by a  
387 strongly supported clade formed by (*Atelopus* + *Oreophrynella*) and (*Frostius* +  
388 *Osornophryne*) that dated back to the Eocene, ca. 37.3 Myr (95% Height Posterior Density  
389 [95% HPD] = 32–42.6) (Fig. 2). The Atlantic Forest genus *Dendrophryniscus* was  
390 recovered as sister to *Amazophrynella*. In turn, this clade was inferred as sister to a clade  
391 encompassing all the remaining bufonid genera, with the divergence between them dating  
392 back to the late Eocene (ca. 36.8 Myr, 95% HPD = 32.6–40.9). The results corroborate an  
393 ancient history of diversification for *Amazophrynella*, dating back to 23 Myr (95% HPD =  
394 19.3–26.6) (Fig. 2).

395 Our phylogenetic results also recovered the monophyly of *Amazophrynella* and two  
396 major clades within the genus (Fig. 2), largely restricted to the western and eastern portions  
397 of Amazonia. The only and noteworthy exception is *A.* OTU22 from the Guiana Shield,

398 recovered as nested within the western clade. The divergence of the western and eastern  
399 clades coincides with the Paleogene–Neogene transition (Oligocene–Miocene ca. 23 Myr;  
400 95% HPD = 19.3–26.6), which is relatively older than most crown ages of other bufonid  
401 genera (Fig. 2). The crown ages of the two major *Amazophrynella* clades both date back to  
402 the middle Miocene, at ca. 14.9 Myr (95% HPD 12.2–17.7) for the western clade and 16.1  
403 Myr (95% HPD = 12.7–19.5) for the eastern clade.

404         In the western clade, northernmost OTUs are nested in a subclade with  
405 representatives of midwestern and southwestern Amazonia, which is sister of a subclade  
406 exclusively composed of OTUs from the southwestern region (Fig. 2). This pattern is  
407 similar within the eastern clade, with OTUs from northeastern Amazonia more closely  
408 related to one of the two subclades distributed in the southeastern region (Fig. 2). Cases of  
409 reciprocal monophyly between OTUs from the northern and southern banks of the Amazon  
410 River were found within both the eastern and western clades. These divergences date back  
411 to the middle Miocene, at ca. 12.2 Myr (95% HPD 9.8–14.6) for the western clade and 13.4  
412 Myr (95% HPD 10.5–16.5) for the eastern clade.

413         Diversification rates slightly differed between the western and eastern clades.  
414 Cladogenesis within the western clade seems to have taken place at a relatively constant  
415 pace, whereas the eastern clade seems to have diversified during a more recent period (late  
416 Miocene; < 10 Myr), mostly within two subclades (Fig. 2). The most recent divergences  
417 occurred in the eastern clade, during the late Pliocene (ca. 2.8–2.9 Myr). In the western  
418 clade, recent divergences are overall older, during the Miocene–Pliocene transition, and  
419 concentrated in northwestern Amazonia (Figs. 1, 2).

420

421 **HISTORICAL BIOGEOGRAPHY**

422 Of the six biogeographic models compared in the ‘BioGeoBEARS’ analyses, the  
423 DIVALIKE+J and DEC+J produced the best statistical fit to the data for the broader and  
424 refined regionalization schemes, respectively (Supporting Information, Table S4). We  
425 interpret the historical biogeography of *Amazophrynella* based on the combination of these  
426 two results (Fig. 3; Supporting Information, Fig. S3). Nevertheless, we also compared the  
427 results obtained by the best-fit models for each partitioning approach without the  
428 consideration of parameter ‘J’, namely the DIVA model for the broader partitioning and  
429 DEC for the refined one (Supporting Information, Table S4).

430         The most recent common ancestor (MRCA) of the genus *Amazophrynella* (ca. 23  
431 Myr, 95% HPD 19.3–26.6) likely occupied the southwestern Amazonia, more specifically  
432 in the interface of the Inambari and Rondonia, which currently corresponds to the area  
433 delimited northward by the upper Amazon River and eastward by the Tapajós River. An  
434 ancient dispersal/vicariance event led to the split between the western and eastern major  
435 clades within the genus. These clades subsequently diversified within distinct areas, along  
436 the Andean foothills in southwestern Amazonia (Inambari) and at the interface of the  
437 Inambari and Rondonia, respectively (Fig. 3; Supporting Information, Fig. S3). Lineages  
438 from the western clade have secondarily dispersed twice northward during the Miocene,  
439 reaching the Napo and ultimately the Imeri regions. This clade has also dispersed toward  
440 the Guiana Shield some 7 Myr (Fig. 3; Supporting Information, Fig. S3). In turn, lineages  
441 within the eastern clade dispersed from around the Inambari and Rondonia regions (western  
442 Brazilian Shield) toward the Guiana Shield during the Miocene (ca. 13.4 Myr, 95% HPD  
443 10.5–16.5), and twice eastward: an older dispersal event at ca. 5.6 Myr (95% HPD 3.8–7.5),  
444 and a more recent event at ca. 3 Myr (95% HPD 1.1–5.8) (Fig. 3; Supporting Information,  
445 Fig. S3). This last dispersal phase displays a stepping-stone pattern, with lineages

446 dispersing from the Rondonia toward the Tapajos, and subsequently east into the Xingu  
447 (Fig. 3; Supporting Information, Fig. S3).

448 Results of the best-fitted models not including the ‘J’ (jump dispersal) parameter  
449 inferred similar ancestral areas relative to models incorporating this parameter (Supporting  
450 Information, Fig. S4). However, by removing the possibility of jump dispersal, the most  
451 probable ancestral areas became more ambiguous. Models without ‘J’ also inferred that the  
452 MRCA of *Amazophrynella* most likely occupied the southwestern Amazonia region  
453 (Supporting Information, Fig. S4), and that a vicariant event led to the split between its  
454 western and eastern major clades in the early Miocene. Vicariant events were also implied  
455 in the split between the Guiana Shield and Brazilian Shield clades (within the eastern  
456 clade), as well as in the diversification events in northwestern Amazonia involving the  
457 Napo and Imeri (Supporting Information, Fig. S4).

458 According to BSM analyses, most of the speciation events within *Amazophrynella*  
459 occurred *in-situ* (i.e., within biogeographic areas), considering both the broad and refined  
460 spatial partitioning ( $29.8 \pm 0.4$  and  $20 \pm 0.8$  events, respectively). For the broad scale  
461 scheme,  $15.4 \pm 0.9$  *in-situ* speciation events have occurred within western Amazonia.  
462 Dispersal events mostly occurred from the Brazilian Shield toward western Amazonia  
463 (Purus–Madeira interfluvium;  $3.3 \pm 0.9$  events). Nevertheless, the Guiana Shield was found to  
464 be the major dispersal receiver resulting in speciation (FE:  $0.8 \pm 0.1$ ).

465 Considering the refined spatial partitioning, the Inambari and Napo harbored the  
466 highest number of *in-situ* speciation events ( $5.4 \pm 1.4$  and  $2.9 \pm 0.9$  events, respectively).  
467 Fewer speciation events occurred in the eastern clade, in which most *in-situ* speciation  
468 occurred within the Brazilian Shield ( $9.4 \pm 0.9$  events). Within the Brazilian Shield, most  
469 *in-situ* speciation events occurred in its westernmost part (Rondonia;  $4.2 \pm 1.2$  events), with

470 a decrease in speciation toward the east, reaching  $1.5 \pm 0.6$  events within the Tapajos and  
471 no speciation within the Xingu (Supporting Information, Table S5). The Andean foothills  
472 (Inambari and Napo) likely acted as the major source of dispersal events within the western  
473 clade ( $0.3 \pm 0.3$  and  $0.3 \pm 0.1$  events, respectively). Within the eastern clade, the Rondonia  
474 and Tapajos likely were the major cores of dispersal events ( $0.3 \pm 0.3$  and  $0.2 \pm 0.2$  events,  
475 respectively) (Supporting Information, Table S5).

476

#### 477 **DIVERSIFICATION THROUGH TIME**

478 Diversification of *Amazophrynella* differed significantly from the expected accumulation of  
479 lineages under a constant diversification model over time ( $\gamma = -2.72, p < 0.01$ ) (Fig. 3c).  
480 Nevertheless, the overall diversification pattern as illustrated by a Lineage Through Time  
481 graph (Fig. 3c) indicates constant diversification (matching the null model) until ca. 4 Myr,  
482 when an increase in cladogenesis occurred. Supporting this pattern of nearly constant  
483 diversification followed by a rapid and relatively recent increase, we found the best-fit  
484 diversification model to be the Yule pure-birth four-rate model. This model showed a  
485 constant rate of lineage accumulation ( $r = 0.17$ ) followed by an increase in diversification  
486 rate ( $r = 0.64$ ) at ca. 4 Myr (Supporting Information, Table S6) and a decrease after ca. 3  
487 Myr ( $r = 0.01$ ). However, the shift in the diversification rate detected ca. 4 Myr is probably  
488 produced by the absence of terminal branches during that time frame which is at least partly  
489 inherent to the DNA-based method of delimitation and thus artifactual, and to the absence  
490 of nominal species that formed recently which could be also related to coarse-grained  
491 taxonomy.

492 **DISCUSSION**

493 **SPECIES DELIMITATION**

494 Our DNA-based species delimitation, which resulted in 22 OTUs on top of the 13 described  
495 species, suggests a vast underestimation of the species richness in *Amazophrynella*. This  
496 underestimation is especially evident in southwestern Amazonia and in the Brazilian  
497 Shield, where more than 70% and 66% of the respective diversity may be not yet formally  
498 described. These observations, along with a pattern of completely non overlapping narrow  
499 geographic ranges, suggest that remaining sampling gaps probably harbor additional  
500 candidate species, notably in Bolivia, Venezuela, Colombia, and southwestern Brazilian  
501 Amazonia (Supporting Information, Fig. S1). Bolivian populations (see De la Riva, 1999)  
502 are of special interest because this region may have acted as a dispersal route between  
503 Amazonia (which eventually gave origin to *Amazophrynella*) and the coastal Atlantic  
504 Forest (*Dendrophryniscus*).

505         The underestimation of species diversity has been repeatedly highlighted in studies  
506 of Amazonian amphibians. A recent estimate found that about 40–50% of the species  
507 inhabiting this region remain to be named and described (Vacher *et al.*, 2020). According to  
508 the present study, this number is even higher for *Amazophrynella* (ca. 62 %). Relative to  
509 other amphibian genera widespread in lowland Amazonia that also started to diversify  
510 during the early Neogene, undescribed diversity within *Amazophrynella* is comparable to  
511 that in *Adenomera* (57%, Fouquet *et al.*, 2014), higher than in *Allobates* (21%; Réjaud *et*  
512 *al.*, 2020) and lower than in *Synapturanus* (83%; Fouquet *et al.*, 2021). Such variation in  
513 unrecognized diversity in clades of similar age may be related to differential ecological  
514 factors and dispersal ability affecting their diversification (Rabosky, 2009; Peterson *et al.*,



515 2011; Miller *et al.*, 2021), but also to the variable effort undertaken on their taxonomic  
516 resolution (Fouquet *et al.*, 2021).

517 Our species delimitation analyses also led to ambiguous OTU boundaries in several  
518 instances, especially among some recently diverging lineages from northwestern  
519 Amazonia. Such discrepancy was likely influenced by the small size of our focal mtDNA  
520 locus and the absence of nuDNA, morphological, and acoustic data (see Miralles & Vences,  
521 2013). Based on these limitations, we advocate caution over strict interpretation of our  
522 delimitation results in the case of such ambiguous boundaries. Nevertheless, the results of  
523 our ancestral area reconstruction analyses should be reliable because most of the conflicting  
524 OTU boundaries involved geographically close populations that occur within the same  
525 broad biogeographic region.

526

#### 527 **LANDSCAPE EVOLUTION INFERRED FROM THE *AMAZOPHRYNELLA* DIVERSIFICATION**

528 The ancestors of the western and eastern major clades of *Amazophrynella* were most likely  
529 respectively isolated along the eastern foothills of the Andes and on the western Brazilian  
530 Shield some 23 Myr. This ancient division of this genus into two major clades at the  
531 Oligocene–Miocene transition was also suggested by previous divergence time analyses  
532 (Rojas *et al.*, 2018). This timeframe is concomitant with the emergence of a vast lacustrine  
533 system and other mega wetlands in western Amazonia, due to the combined effect of the  
534 uplift of the Andean mountain range and a western depression of the continental plate  
535 (Hoorn *et al.*, 2010; Bicudo *et al.*, 2019). These mega wetland systems may have acted as  
536 relevant geographical barriers by segregating populations strongly associated with *terra*  
537 *firme* forests and narrow ecological niche breadth (Hoorn *et al.*, 2010), as is the case of  
538 *Amazophrynella* spp. Such a pattern of ancient lineage segregation between western and

539 eastern lineages is also evident in the diversification history of other Amazonian groups,  
540 like the anuran genera *Allobates* (Réjaud *et al.*, 2020) and *Adenomera* (Fouquet *et al.*,  
541 2014) and lizard genera *Alopoglossus* (Ribeiro-Júnior *et al.*, 2020), *Kentropyx* (Sheu *et al.*,  
542 2020), and *Chatogekko* (Geurgas & Rodrigues, 2010).

543         Within each of the two major clades of *Amazophrynella*, we found a consistent  
544 pattern of northern Amazonian subclades originating through dispersal events from  
545 southern Amazonia, before the establishment of the transcontinental Amazon River (10–9  
546 Myr according to Hoorn *et al.*, 2010, 2017 or 5–3 Myr according to Latrubesse *et al.*,  
547 2010). This contradicts a previous biogeographic interpretation that attributed these splits to  
548 a vicariant event triggered by the emergence of the Amazon River (Rojas *et al.*, 2018).  
549 Nevertheless, the diversification history of *Amazophrynella* still suggests a major role of  
550 the Amazon River as a secondary geographical barrier, as the establishment of this river  
551 likely limited the dispersion and genetic interchange between northern and southern  
552 populations since the middle Miocene. This timing is therefore consistent with the “old  
553 origin” hypothesis for the establishment of the Amazon River (Hoorn *et al.*, 2010, 2017).  
554 This riverine barrier may have favored *in-situ* diversification throughout northern and  
555 southern Amazonia, mirroring what has been suggested for the effects of large rivers on the  
556 diversification of *terra firme* Amazonian birds (Naka & Brumfield, 2018).

557         During the middle Miocene (ca. 15–10 Myr), the western clade of *Amazophrynella*  
558 underwent an initial diversification along the southern part of the Andean foothills and  
559 progressively dispersed toward the north and diversified northward. This is concomitant  
560 with the uplift of the Fitzcarrald Arch and the southwestern to northwestern perimontane  
561 accumulation of Andean sediment as a result of continuous orogeny (Espurt *et al.*, 2010;  
562 Hoorn *et al.*, 2010). Both events may have facilitated *Amazophrynella* range expansion due

563 to the development of *terra firme* forests in westernmost Amazonia. At the same time, the  
564 eastern clade also expanded its range to the east and north into the Guiana Shield, the latter  
565 probably via an upland route connecting these regions (Purus Arch) (Hoorn *et al.*, 2010).  
566 The west-east inversion of the Amazon watershed (Hoorn *et al.*, 2010, 2017; Latrubesse *et*  
567 *al.*, 2010) ultimately prevented any further dispersals between the Guiana Shield and  
568 Brazilian Shield. Similar to the western clade, east- and northward range expansions within  
569 the eastern clade were concomitant with the demise of mega wetlands and the development  
570 of *terra firme* forests (Bicudo *et al.*, 2019).

571       Posterior diversification events within *Amazophrynella* (< 10 Myr) include the  
572 unexpected dispersal of a lineage embedded within the western subclade into the Guiana  
573 Shield during the late Miocene (ca. 7 Myr). This apparently long dispersion event may be  
574 explained by possible extinction of intervening populations, or simply by a bias of  
575 undersampling. Either way, it implies a trans-Amazonian dispersal, considering that this  
576 river was already established at that time (*sensu* Hoorn *et al.*, 2010, 2017). Considering that  
577 internal areas of the western sedimentary basin are only recently more suitable for the  
578 expansion of *terra firme* lineages such as *Amazophrynella* (Pupim *et al.*, 2019), this  
579 dispersal event may have occurred via a northwestern route, possibly through the Vaupes  
580 Arch, a concomitant northern watershed connecting the uplands of western and eastern  
581 Amazonia (Mora *et al.*, 2010). In fact, given the strong habitat association of this genus, the  
582 western clade diversification is consistent with progressive development of *terra firme*  
583 forests towards the east, as a result of continuous Andean sediment influx and lowering of  
584 the river channels after the demise of the lacustrine systems (Pupim *et al.*, 2019). This is  
585 also supported by the fact that the most recent lineages of the western clade are confined to  
586 the region once filled by the mega wetland systems, corroborating the pattern observed in

587 other amphibian diversification histories (Fouquet *et al.*, 2014; Réjaud *et al.*, 2020) and a  
588 concentration of recent and phylogenetically closer bird lineages in this region (Bicudo *et*  
589 *al.*, 2019; Crouch *et al.*, 2019). It is also noteworthy that, even though the undersampling of  
590 Amazonia hampers firm interpretation (Vacher *et al.*, 2020), *Amazophrynella* populations  
591 are possibly absent from the innermost western Amazonia sedimentary basin (Supporting  
592 Information, Fig. S1), where *terra firme* forests are more recent (Pupim *et al.*, 2019). In  
593 addition, no *Amazophrynella* population has been reported to date from the Branco River  
594 basin and the easternmost Solimões-Negro interfluvium (Supporting Information, Fig. S1), the  
595 latest being considered as an area of endemism for birds (Jaú; Borges & Silva, 2012). A  
596 combination of recent development of *terra firme* forests and prevalence of more open  
597 habitats in this region (Adeney *et al.*, 2016), as well as the existence of a riverine barrier  
598 connecting the Japurá River to the Negro River until very recently (ca. 1,000 years ago;  
599 Ruokolainen *et al.*, 2019), may have prevented the range expansion of the western clade of  
600 *Amazophrynella* into the innermost northwestern Amazonia.

601         Conversely, the Eastern subclade broadly expanded its range to the east during the  
602 same timeframe as the western clade (< 10 Myr). Instead of a greater geomorphological  
603 influence controlling the development of *terra firme* forests, major changes in vegetation  
604 cover in this region have been especially affected by climatic variations over time, with  
605 drier glacial periods likely changing the structure of forests (Cheng *et al.*, 2013).  
606 *Amazophrynella* have possibly dispersed eastward following humid forest development  
607 during favorable climatic conditions. However, they maintained low diversification rates  
608 until ca. 6–5 Myr, when the putative combined influence of drainage rearrangements of the  
609 tributaries of the Amazon River (Latrubesse, 2002; Rossetti, 2014; Hayakawa & Rossetti,  
610 2015; Moraes *et al.*, 2020) and cyclical unfavorable climatic conditions (Cheng *et al.*,

611 2013) may have promoted a rapid accumulation of new lineages. These factors may also  
612 explain a higher stasis on the diversification of the Guiana Shield clade over time, as this  
613 region currently presents a lower occurrence of large tributaries of the Amazon River and  
614 has been geomorphologically more stable over time (Bicudo *et al.*, 2019).

615

#### 616 **ECOLOGICAL CONSERVATISM AND DIVERSIFICATION RATES**

617 Increasing diversification rates are generally associated with the acquisition of evolutionary  
618 novelties that allow the exploration of new ecological opportunities (Erwin, 2015).

619 Therefore, the nearly continuous and stable diversification rate seen in *Amazophrynella* is  
620 in accordance with its extreme phenotypic conservatism and overall conserved ecology  
621 (Rojas *et al.*, 2018). Even with the putative new ecological opportunities arising from the  
622 dynamic Amazonian landscape evolution of the Miocene, such conservatism most likely  
623 limited *Amazophrynella* dispersal and possibly fostered lineage extinction in unsuitable  
624 regions (Rabosky, 2009; Peterson *et al.*, 2011).

625 [Biogeographic studies using Amazonian amphibians as model systems commonly](#)  
626 [support ancient timeframes for their initial diversification \(e.g., Santos \*et al.\*, 2009;](#)  
627 [Castroviejo-Fisher \*et al.\*, 2014; Fouquet \*et al.\*, 2014; Sá \*et al.\*, 2019; Réjaud \*et al.\*, 2020;](#)  
628 [Fouquet \*et al.\*, 2021\), and this is also the case for \*Amazophrynella\*. Such ancient](#)  
629 [timeframes are somewhat incongruent with the relatively more recent ones reported for](#)  
630 [other vertebrates, such as some birds \(e.g., Silva \*et al.\*, 2019\) and primates \(e.g., Alfaro \*et\*](#)  
631 [al., 2015\), but also for other amphibians \(e.g., Jaramillo \*et al.\*, 2020\). Changes in the](#)  
632 [permeability of riverine barriers until recently \(Plio-Pleistocene\) may have led to a](#)  
633 [relatively higher frequency of dispersal events in the evolutionary history of vertebrate](#)  
634 [groups with higher vagility, which may also have involved continuous adaptation to](#)

635 different habitats (Smith *et al.*, 2014; Pirani *et al.*, 2019). These processes may explain  
636 higher and more recent lineage accumulation during the Neogene for these groups  
637 compared to ecologically conserved and dispersal-limited amphibians. Therefore, based on  
638 the evidence for *Amazophrynella*, we suggest that a combination of narrow habitat  
639 associations and greater dispersal limitation led to stronger signatures of ancient landscape  
640 changes on the history of biological diversification.

641

## 642 **CONCLUSION**

643 In summary, our results provide a reevaluation of species richness within *Amazophrynella*  
644 and their respective distributions. Moreover, they provide insights on the historical  
645 biogeography of these tiny toads, which is consistent with proposed landscape changes in  
646 Amazonia throughout Neogene. Given the extreme ecological association of  
647 *Amazophrynella* with *terra firme* forests, our results corroborate most of the hypothesized  
648 spatial and temporal evolution of these habitats across the Amazonian landscape. The  
649 historical biogeography of *Amazophrynella* largely agrees with a progressive transition of  
650 lacustrine and fluviotidal systems to *terra firme* forest habitats at western Amazonia during  
651 the Neogene, as well as to a Miocene origin of the transcontinental Amazon River. These  
652 results reinforce the perception that ancient Amazonian landscape changes, such as the  
653 emergence of broad western lacustrine ecosystems and the longitudinal drainage transition,  
654 had a major impact on the diversification of terrestrial vertebrates.

**655 ACKNOWLEDGEMENTS**

656 This study benefited from an “Investissement d’Avenir” grant managed by the Agence  
657 Nationale de la Recherche (CEBA, ANR-10-LABX-25-01; TULIP, ANR-10-LABX-0041;  
658 ANAEE-France, ANR-11-INBS-0001), and the French/Brazilian GUYAMAZON program  
659 (IRD, CNRS, CTG, CIRAD and Fundação de Amparo à Pesquisa do Estado do Amazonas-  
660 FAPEAM; #062.00962/2018), co-coordinated by AF and FPW. LJCLM thanks  
661 Coordenação de Aperfeiçoamento de Pessoal de Nível Superior-CAPES for a scholarship  
662 (#88887.630472/2021-00). MTR thanks Conselho Nacional de Desenvolvimento Científico  
663 e Tecnológico (CNPq), Fundação de Amparo à Pesquisa do Estado de São Paulo (FAPESP;  
664 grants: #2003/10335-8, #2011/50146-6), and NSF-FAPESP Dimensions of Biodiversity  
665 Program (grants: BIOTA #2013/50297-0, NSF-DEB #1343578) and NASA. SRR  
666 acknowledges a grant from SENESCYT (Arca de Noé Initiative). FPW thanks CNPq  
667 (Productivity Fellowship), CAPES (Visiting Professor Fellowship), FAPEAM, and the  
668 L’Oréal-UNESCO for Women in Science Program. PJRK thanks the Fonds voor  
669 Wetenschappelijk Onderzoek (grants FWO12A7614N and FWO12A7617N). We thank B.  
670 Noonan (UM), T. Grant (USP), D. Dittmann (LSU), J. Gomes (MPEG), T. C. Ávila-Pires  
671 (MPEG), S. Katanova (AMNH), D. A. Kizirian (AMNH), A. Crawford (UNIANDÉS), J.  
672 M. Padial (AMNH), A. A Silva, C. C. Ribas and M. Freitas (INPA), and S. Castroviejo-  
673 Fisher (PUCRS) for their contribution with material used in this work, and S. Manzi and U.  
674 Suescun for their help in the laboratory procedures. We are also thankful to L. Pinheiro  
675 (UFPA), Amy Lathrop (ROM), C. Spencer (MVZ), A. Acosta Galvis (IAvH-Am), J.  
676 Courtois (MNHN), and A. Ohler (MNHN) for providing relevant information on museum  
677 specimens; and to Igor L. Kaefer (UFAM) for kindly sharing the original material  
678 sequenced for *A. bilinguis*.

679 **REFERENCES**

680 **Adeney JM, Christensen NL, Vicentini A, Cohn-Haft M. 2016.** White-sand ecosystems  
681 in Amazonia. *Biotropica* **48**: 7–23.

682 **Albert JS, Val P, Hoorn C. 2018.** The changing course of the Amazon River in the  
683 Neogene: Center stage for Neotropical diversification. *Neotropical Ichthyology* **16**:  
684 e180033.

685 **Alfaro JWL, Boubli JP, Paim FP, Ribas CC, da Silva MNF, Messias M., Röhe F,**  
686 **Mercês MP, Silva Júnior JS, Silva CR, Pinho GM, Koshkariank G, Nguyenk**  
687 **MTT, Harada ML, Rabelo RM, Queiroz HL, Alfaro ME, Farias IP. 2015.**  
688 Biogeography of squirrel monkeys (genus *Saimiri*): South-central Amazon origin and  
689 rapid pan-Amazonian diversification of a lowland primate. *Molecular Phylogenetics*  
690 *and Evolution* **82**: 436–454.

691 **Antonelli A., Sanmartín I. 2011.** Why are there so many plant species in the Neotropics?  
692 *Taxon* **60**: 403–414.

693 **Antonelli A., Ariza M, Albert J, Andermann T, Azevedo J, Bacon C, Faurby S,**  
694 **Guedes T, Hoorn C, Lohmann LG, Matos-Maraví P, Ritter CD, Sanmartín I,**  
695 **Silvestro D, Tejedor M, ter Steege H, Tuomisto H, Werneck FP, Zizka A,**  
696 **Edwards S. 2018.** Conceptual and empirical advances in Neotropical biodiversity  
697 research. *PeerJ* **6**: e5644.

698 **Bicudo TC, Sacek V, Almeida RPD, Bates JM, Ribas CC. 2019.** Andean tectonics and  
699 mantle dynamics as a pervasive influence on Amazonian ecosystem. *Scientific*  
700 *Reports* **9**: 1–11.

701 **Borges SH, Silva JMC. 2012.** A new area of endemism for Amazonian birds in the Rio  
702 Negro basin. *Wilson Journal of Ornithology* **124**: 15–24.



- 703 **Bouckaert R, Heled J, Kühnert D, Vaughan T, Wu C-H, Xie D, Suchard MA,**  
704 **Rambaut A, Drummond AJ. 2014.** BEAST 2: A Software Platform for Bayesian  
705 Evolutionary Analysis. *PLOS Computational Biology* **10**: e1003537.
- 706 **Castroviejo-Fisher S, Guayasamin JM, Gonzalez-Voyer A, Vilà C. 2014.** Neotropical  
707 diversification seen through glassfrogs. *Journal of Biogeography* **41**: 66–80.
- 708 **Cheng H, Sinha A, Cruz FW, Wang X, Edwards RL, D’Horta FM, Ribas CC, Vuille**  
709 **M, Stott LD, Auler AS. 2013.** Climate change patterns in Amazonia and  
710 biodiversity. *Nature Communications* **4**: 1411.
- 711 **Cracraft J. 1985.** Historical biogeography and patterns of differentiation within the South  
712 American avifauna: areas of endemism. *Ornithological Monographs* **36**: 49–84.
- 713 **Crouch NMA, Capurucho JMG, Hackett SJ, Bates JM. 2019.** Evaluating the  
714 contribution of dispersal to community structure in Neotropical passerine birds.  
715 *Ecography* **42**: 390–399.
- 716 **De la Riva I. 1999.** First record of *Dendrophryniscus minutus* (Melin, 1941) in Bolivia.  
717 *Herpetozoa* **12**: 91–92.
- 718 **Drummond AJ, Ho SYW, Phillips MJ, Rambaut A. 2006.** Relaxed phylogenetics and  
719 dating with confidence. *PLoS Biology* **4**: e88.
- 720 **Duellman WE. 1979.** *The South American herpetofauna: Its origin, evolution, and*  
721 *dispersal*. Kansas: Museum of Natural History/University of Kansas.
- 722 **Dupin J, Matzke NJ, Sarkinen T, Knapp S, Olmstead R, Bohs L, Smith S. 2017.**  
723 Bayesian estimation of the global biogeographic history of the Solanaceae. *Journal of*  
724 *Biogeography* **44**: 887–899.
- 725 **Erwin DH. 2015.** Novelty and innovation in the history of life. *Current Biology* **25**: R930–  
726 R940.

- 727 **Espurt N, Baby P, Brusset S, Roddaz M, Hermoza W, Barbarand J. 2010.** The Nazca  
728 Ridge and uplift of the Fitzcarrald Arch: implications for regional geology in northern  
729 South America. In: Hoorn C, Wesselingh FP, eds. *Amazonia: landscape and species*  
730 *evolution. A look into the past*. Chichester: Wiley-Blackwell, 89–100.
- 731 **Ezard T, Fujisawa T, Barraclough T. 2009.** splits: SPecies' Limits by Threshold  
732 Statistics. R package version 1.0-11/r29.
- 733 **Feng YJ, Blackburn DC, Liang D, Hillis DM, Wake DB, Cannatella DC, Zhang P.**  
734 2017. Phylogenomics reveals rapid, simultaneous diversification of three major  
735 clades of Gondwanan frogs at the Cretaceous-Paleogene boundary. *PNAS* **114**: 5864–  
736 5870.
- 737 **Fouquet A, Gilles A, Vences M, Marty C. 2007.** Underestimation of species richness in  
738 Neotropical frogs revealed by mtDNA analyses. *PLoS ONE* **2**: e1109.
- 739 **Fouquet A, Recoder R, Teixeira Jr M., Cassimiro J, Amaro R, Camacho A,**  
740 **Damasceno R, Carnaval AC, Moritz C, Rodrigues MT. 2012a.** Molecular  
741 phylogeny and morphometric analyses reveal deep divergence between Amazonia  
742 and Atlantic Forest species of *Dendrophryniscus*. *Molecular Phylogenetics and*  
743 *Evolution* **62**: 826–838.
- 744 **Fouquet A, Loebmann D, Castroviejo-Fisher S, Padial JM, Orrico VGD, Lyra M,**  
745 **Roberto I J, Kok, PJR, Haddad CFB, Rodrigues MT. 2012b.** From Amazonia to  
746 the Atlantic forest: Molecular phylogeny of Physelaphryninae frogs reveals  
747 unexpected diversity and a striking biogeographic pattern emphasizing conservation  
748 challenges. *Molecular Phylogenetics and Evolution* **65**: 547–561.
- 749 **Fouquet A, Cassini C, Haddad CFB, Pech N, Rodrigues MT. 2014.** Species  
750 delimitation, patterns of diversification and historical biogeography of a Neotropical

751 frog genus *Adenomera* (Anura, Leptodactylidae). *Journal of Biogeography* **41**: 855–  
752 870.

753 **Fouquet A, Leblanc K, Framit M, Réjaud A, Rodrigues MT, Castroviejo-Fisher S,**  
754 **Peloso PLV, Prates I, Manzi S, Suescun U, Baroni S, Moraes LJCL, Recoder R,**  
755 **Marques-Souza S, Dal-Vecchio F, Camacho A, Guellere JM, Rojas-Runjaic**  
756 **FJM, Gagliardi-Urrutia G, Carvalho VT, Gordo M, Kok PJR., Hrbek T,**  
757 **Werneck FP, Crawford AJ, Ron SR, Mueses-Cisneros JJ, Zamora RRR, Pavan**  
758 **D, Simões PI, Ernst R, Fabre AC. 2021a.** Species diversity and biogeography of an  
759 ancient frog clade from the Guiana Shield (Anura: Microhylidae: *Adelastes*,  
760 *Otophryne*, *Synapturanus*) exhibiting spectacular phenotypic diversification.  
761 *Biological Journal of the Linnean Society* **132**: 233–256.

762 **Fujisawa T, Barraclough TG. 2013.** Delimiting species using single-locus data and the  
763 Generalized Mixed Yule Coalescent (GMYC) approach: a revised method and  
764 evaluation on simulated datasets. *Systematic Biology* **62**: 707–724.

765 **Funk WC, Caminer M, Ron SR. 2012.** High levels of cryptic species diversity uncovered  
766 in Amazonian frogs. *Proceedings of the Royal Society B: Biological Sciences* **279**:  
767 1806–1814.

768 **Gernhard T. 2008.** The conditioned reconstructed process. *Journal of Theoretical Biology*  
769 **253**: 769–778.

770 **Geurgas SR, Rodrigues MT. 2010.** The hidden diversity of *Coleodactylus amazonicus*  
771 (Sphaerodactylinae, Gekkota) revealed by molecular data. *Molecular Phylogenetics*  
772 *and Evolution* **54**: 583–593.

- 773 **Godinho MB, da Silva FR. 2018.** The influence of riverine barriers, climate, and  
774 topography on the biogeographic regionalization of Amazonian anurans. *Scientific*  
775 *Reports* **8**: 1–11.
- 776 **Hayakawa EH, Rossetti, DF. 2015.** Late quaternary dynamics in the Madeira river basin,  
777 southern Amazonia (Brazil), as revealed by paleomorphological analysis. *Anais da*  
778 *Academia Brasileira de Ciências* **87**: 29–49.
- 779 **Hime PM, Lemmon AR, Lemmon ECM, Prendini E, Brown JM, Thomson RC,**  
780 **Kratovil JD, Noonan BP, Pyron RA, Peloso PLV, Kortyna ML, Keogh JS,**  
781 **Donnellan SC, Mueller RL, Raxworthy CJ, Kunte K, Ron SR, Das S, Gaitonde**  
782 **N, Green DM, Labisko J, Che J, Weisrock DW. 2021.** Phylogenomics reveals  
783 ancient gene tree discordance in the amphibian tree of life. *Systematic Biology* **70**:  
784 49–66.
- 785 **Horn C, Wesselingh FP, ter Steege H, Bermudez MA, Mora A, Sevink J, Sanmartín**  
786 **I, Sanchez-Meseguer A, Anderson CL, Figueiredo JP, Jaramillo C, Riff D, Negri**  
787 **FR, Hooghiemstra H, Lundberg J, Stadler T, Särkinen T, Antonelli A. 2010.**  
788 Amazonia through time: Andean uplift, climate change, landscape evolution, and  
789 biodiversity. *Science* **330**: 927–931.
- 790 **Horn C, Bogotá-A GR, Romero-Baez M, Lammertsma EI, Flantua SGA, Dantas EL,**  
791 **Dino R, Chemale Jr F. 2017.** The Amazon at sea: Onset and stages of the Amazon  
792 River from a marine record, with special reference to Neogene plant turnover in the  
793 drainage basin. *Global and Planetary Change* **153**: 51–65.
- 794 **Hurvich CM, Tsai CL. 1989.** Regression and time series model selection in small  
795 samples. *Biometrika* **76**: 297–307.

- 796 **Jaramillo AF, De la Riva I, Guayasamin JM, Chaparro JC, Gagliardi-Urrutia G,**  
797 **Gutiérrez RC, Brcko I, Vilà C, Castroviejo-Fisher S. 2020.** Vastly underestimated  
798 species richness of Amazonian salamanders (Plethodontidae: *Bolitoglossa*) and  
799 implications about plethodontid diversification. *Molecular Phylogenetics and*  
800 *Evolution* **149**: 106841.
- 801 **Kaefer IL, Rojas RR, Ferrão M, Farias IP, Lima AP. 2019.** A new species of  
802 *Amazophrynella* (Anura: Bufonidae) with two distinct advertisement calls. *Zootaxa*  
803 **4577**: 316–334.
- 804 **Kapli P, Lutteropp S, Zhang J, Kobert K, Pavlidis P, Stamatakis A, Flouri T. 2017.**  
805 Multi-rate Poisson tree processes for single-locus species delimitation under  
806 maximum likelihood and Markov chain Monte Carlo. *Bioinformatics* **33**: 1630–1638.
- 807 **Katoh K, Standley DM. 2013.** MAFFT Multiple Sequence Alignment Software Version 7:  
808 Improvements in Performance and Usability. *Molecular Biology and Evolution* **30**:  
809 772–780.
- 810 **Kearse M, Moir R, Wilson A, Stones-Havas S, Cheung M, Sturrock S, Buxton S,**  
811 **Cooper A, Markowitz S, Duran C, Thierer T, Ashton B, Meintjes P, Drummond**  
812 **A. 2012.** Geneious Basic: an integrated and extendable desktop software platform for  
813 the organization and analysis of sequence data. *Bioinformatics* **28**: 1647–1649.
- 814 **Kok PJR, Russo VG, Ratz S, Means DB, MacCulloch RD, Lathrop A, Aubret F,**  
815 **Bossuyt F. 2017.** Evolution in the South American “Lost World”: insights from  
816 multilocus phylogeography of stefanias (Anura, Hemiphraetidae, *Stefania*). *Journal*  
817 *of Biogeography* **44**: 170–181.
- 818 **Kok PJR, Ratz S, MacCulloch RD, Lathrop A, Dezfoulian R, Aubret F, Means DB.**  
819 **2018.** Historical biogeography of the palaeoendemic toad genus *Oreophrynella*

- 820 (Amphibia: Bufonidae) sheds a new light on the origin of the Pantepui endemic  
821 terrestrial biota. *Journal of Biogeography* **45**: 26–36.
- 822 **Kumar S, Stecher G, Tamura K. 2016.** MEGA7: Molecular Evolutionary Genetics  
823 Analysis version 7.0 for bigger datasets. *Molecular Biology and Evolution* **33**: 1870–  
824 1874.
- 825 **Klaus KV, Matzke NJ. 2020.** Statistical Comparison of Trait-Dependent Biogeographical  
826 Models Indicates That Podocarpaceae Dispersal Is Influenced by Both Seed Cone  
827 Traits and Geographical Distance. *Systematic Biology* **69**: 61–75.
- 828 **Landis MJ, Matzke NJ, Moore BR, Huelsenbeck JP. 2013.** Bayesian analysis of  
829 biogeography when the number of areas is large. *Systematic Biology* **62**: 789–804.
- 830 **Lanfear R, Frandsen PB, Wright AM, Senfeld T, Calcott B. 2017.** PartitionFinder 2:  
831 New methods for selecting partitioned models of evolution for molecular and  
832 morphological phylogenetic analyses. *Molecular Biology and Evolution* **34**: 772–773.
- 833 **Latrubesse EM. 2002.** Evidence of Quaternary palaeohydrological changes in middle  
834 Amazônia: TheAripuanã-Roosevelt and Jiparaná “fans”. *Zeitschrift für*  
835 *Geomorphologie (neue folge)* **129**: 61–72.
- 836 **Latrubesse EM, Cozzuol M, da Silva-Caminha SAF, Rigsby CA, Absy ML, Jaramillo**  
837 **C. 2010.** The Late Miocene palaeogeography of the Amazon Basin and the evolution  
838 of the Amazon River system. *Earth-Science Reviews* **99**: 99–124.
- 839 **Leite RN, Rogers DS. 2013.** Revisiting Amazonian phylogeography: insights into  
840 diversification hypotheses and novel perspectives. *Organisms Diversity & Evolution*  
841 **13**: 639–664.
- 842 **Luo A, Ling C, Ho SYW, Zhu CD. 2017.** Comparison of methods for molecular species  
843 delimitation across a range of speciation scenarios. *Systematic Biology* **67**: 830–846.

- 844 **Mângia S, Koroiva R, Santana DJ. 2020.** A new tiny toad species of *Amazophrynella*  
845 (Anura: Bufonidae) from east of the Guiana Shield in Amazonia, Brazil. *PeerJ* **8:**  
846 e9887.
- 847 **Marques-Souza S, Pellegrino KCM, Brunes TO, Carnaval AC, Damasceno RP,**  
848 **Borges MLO, Gallardo CC, Rodrigues MT. 2020.** Hidden in the DNA: insights on  
849 how multiple historical processes and natural history traits shaped patterns of cryptic  
850 diversity in an Amazon leaf-litter lizard *Loxopholis osvaldoi* (Squamata:  
851 Gymnophthalmidae). *Journal of Biogeography* **47:** 501–515.
- 852 **Matzke NJ. 2013.** BioGeoBEARS: biogeography with Bayesian (and likelihood)  
853 evolutionary analysis in R scripts. R Package, Version 0.2, 1, 2013.
- 854 **McCormack JE, Heled J, Delaney KS, Peterson AT, Knowles LL. 2011.** Calibrating  
855 divergence times on species trees versus gene trees: Implications for speciation  
856 history of *Aphelocoma* jays. *Evolution* **65:** 184–202.
- 857 **Miller MJ, Bermingham E, Turner BL, Touchon JC, Johnson AB, Winker K. 2021.**  
858 Demographic consequences of foraging ecology explain genetic diversification in  
859 Neotropical bird species. *Ecology Letters* **24:** 563–571.
- 860 **Miralles A, Vences M. 2013.** New metrics for comparison of taxonomies reveal striking  
861 discrepancies among species delimitation methods in *Madascincus* lizards. *PLoS*  
862 *ONE* **8:** e68242.
- 863 **Mora A, Baby P, Roddaz M, Parra M, Brusset S, Hermoza W, Espurt N. 2010.**  
864 Tectonic history of the Andes and sub-Andean zones: implications for the  
865 development of the Amazon drainage basin. In: Hoorn C, Wesselingh FP, eds.  
866 *Amazonia: landscape and species evolution. A look into the past.* Chichester: Wiley–  
867 Blackwell, 38–60.

- 868 **Moraes LJCL, Pavan D, Barros MC, Ribas CC. 2016.** The combined influence of  
869 riverine barriers and flooding gradients on biogeographical patterns for amphibians  
870 and squamates in south-eastern Amazonia. *Journal of Biogeography* **43**: 2113–2124.
- 871 **Moraes LJCL, Ribas CC, Pavan D, Werneck FP. 2020.** Biotic and landscape evolution  
872 in an Amazonian contact zone: insights from the herpetofauna of the Tapajós River  
873 basin. In: Rull V, Carnaval AC, eds. *Neotropical Diversification: Patterns and*  
874 *Processes*. Berlin: Springer, 683–712.
- 875 **Naka LN, Brumfield RT. 2018.** The dual role of Amazonian rivers in the generation and  
876 maintenance of avian diversity. *Science Advances* **4**: eaar8575.
- 877 **Oliveira U, Vasconcelos MF, Santos AJ. 2017.** Biogeography of Amazon birds: rivers  
878 limit species composition, but not areas of endemism. *Scientific Reports* **7**: 2992.
- 879 **Padial JM, Miralles A, De la Riva I, Vences M. 2010.** The integrative future of  
880 taxonomy. *Frontiers in Zoology* **7**: 1–14.
- 881 **Paradis E, Claude J, Strimmer K. 2004.** APE: analyses of phylogenetics and evolution in  
882 R language. *Bioinformatics* **20**: 289–290.
- 883 **Paz A, Crawford AJ. 2012.** Molecular-based rapid inventories of sympatric diversity: a  
884 comparison of DNA barcode clustering methods applied to geography-based vs  
885 clade-based sampling of amphibians. *Journal of Biosciences* **37**: 887–896.
- 886 **Peterson AT, Soberón J, Pearson RG, Anderson RP, Martínez-Meyer E, Nakamura**  
887 **M, Araújo MB. 2011.** *Ecological niches and geographic distributions (MPB-49)*  
888 (Vol. 49). New Jersey: Princeton University Press.
- 889 **Pirani RM, Werneck FP, Thomaz AT, Kenney ML, Sturaro MJ, Ávila-Pires TCS,**  
890 **Peloso P LV, Rodrigues MT, Knowles LL. 2019.** Testing main Amazonian rivers as



- 891 barriers across time and space within widespread taxa. *Journal of Biogeography* **46**:  
892 2444–2456.
- 893 **Pirani RM, Peloso PL, Prado JR, Polo ÉM, Knowles LL, Ron SR, Rodrigues MT,**  
894 **Sturaro MJ, Werneck FP. 2020.** Diversification history of clown tree frogs in  
895 Neotropical rainforests (Anura, Hylidae, *Dendropsophus leucophyllatus* group).  
896 *Molecular Phylogenetics and Evolution* **150**: 106877.
- 897 **Puillandre N, Brouillet S, Achaz G. 2021.** ASAP: assemble species by automatic  
898 partitioning. *Molecular Ecology Resources* **21**: 609–620.
- 899 **Pupim FN, Sawakuchi AO, Almeida RP, Ribas CC, Kern AK, Hartmann GA, Chiessi**  
900 **CM, Tamura LN, Mineli TD, Savian JF, Grohmann CH, Bertassoli Jr. DJ, Stern**  
901 **AG, Cruz FW, Cracraft J. 2019.** Chronology of Terra Firme formation in  
902 Amazonian lowlands reveals a dynamic Quaternary landscape. *Quaternary Science*  
903 *Reviews* **210**: 154–163.
- 904 **Pybus OG, Harvey PH. 2000.** Testing macro-evolutionary models using incomplete  
905 molecular phylogenies. *Proceedings of the Royal Society B: Biological Sciences* **267**:  
906 2267–2272.
- 907 **Rabosky DL. 2006.** LASER: A Maximum Likelihood toolkit for detecting temporal shifts  
908 in diversification rates from molecular phylogenies. *Evolutionary Bioinformatics* **2**:  
909 117693430600200.
- 910 **Rabosky DL. 2009.** Ecological limits and diversification rate: alternative paradigms to  
911 explain the variation in species richness among clades and regions. *Ecology Letters*  
912 **12**: 735–743.

- 913 **Rambaut A, Drummond AJ, Xie D, Baele G, Suchard MA. 2018.** Posterior  
914 summarisation in Bayesian phylogenetics using Tracer 1.7. *Systematic Biology* **67**:  
915 901–904.
- 916 **Ratnasingham S, Hebert PDN. 2013.** A DNA-based registry for all animal species: the  
917 Barcode Index Number (BIN) system. *PLoS ONE* **8**: e66213.
- 918 **Ree RH, Smith SA. 2008.** Maximum Likelihood inference of geographic range evolution  
919 by dispersal, local extinction, and cladogenesis. *Systematic Biology* **57**: 4–14.
- 920 **Ree RH, Sanmartín I. 2018.** Conceptual and statistical problems with the DEC+J model  
921 of founder–event speciation and its comparison with DEC via model selection.  
922 *Journal of Biogeography* **45**: 741–749.
- 923 **Réjaud A, Rodrigues MT, Crawford AJ, Castroviejo-Fisher S, Jaramillo AF,**  
924 **Chaparro JC, Glaw F, Gagliardi-Urrutia G, Moravec J, De la Riva IJ, Perez P,**  
925 **Lima AP, Werneck FP, Hrbek T, Ron SR, Ernst R, Kok PJR, Driskell A, Chave**  
926 **J, Fouquet A. 2020.** Historical biogeography identifies a possible role of the Pebas  
927 system in the diversification of the Amazonian rocket frogs (Aromobatidae:  
928 *Allobates*). *Journal of Biogeography* **47**: 2472–2482.
- 929 **Ribeiro-Júnior MA, Choueri E, Lobos S, Venegas P, Torres-Carvajal O, Werneck FP.**  
930 **2020.** Eight in one: morphological and molecular analyses reveal cryptic diversity in  
931 Amazonian alopoglossid lizards (Squamata: Gymnophthalmoidea). *Zoological*  
932 *Journal of the Linnean Society* **190**: 227–270.
- 933 **Ronquist F. 1997.** Dispersal–vicariance analysis: A new approach to the quantification of  
934 historical biogeography. *Systematic Biology* **46**: 195–203.
- 935 **Rossetti DF. 2014.** The role of tectonics in the late Quaternary evolution of Brazil’s  
936 Amazonian landscape. *Earth-Science Reviews* **139**: 362–389.

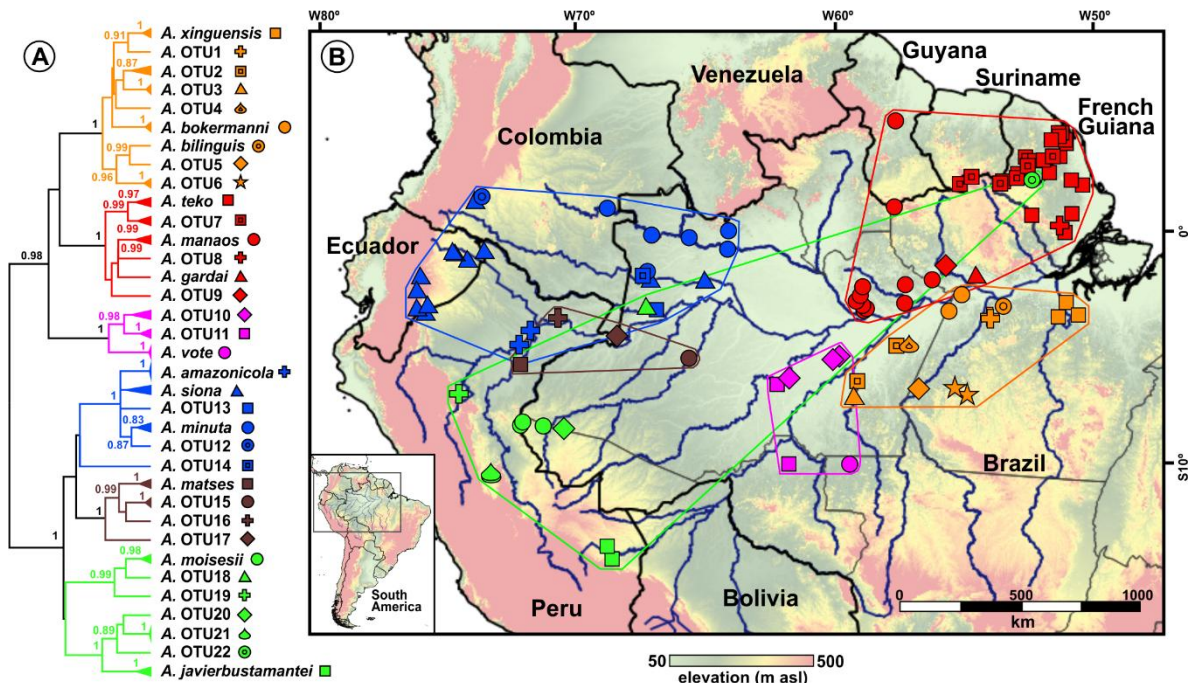
- 937 **Rojas RR, Fouquet A, Ron SR, Hernández-Ruz EJ, Melo-Sampaio PR, Chaparro JC,**  
938 **Vogt RC, de Carvalho VT, Pinheiro LC, Ávila RW, Farias IP, Gordo M, Hrbek**  
939 **T. 2018.** A Pan-Amazonian species delimitation: high species diversity within the  
940 genus *Amazophrynella* (Anura: Bufonidae). *PeerJ* **6**: 1–56.
- 941 **Rull V. 2011.** Neotropical biodiversity: timing and potential drivers. *Trends in Ecology &*  
942 *Evolution* **26**: 508–513.
- 943 **Ruokolainen K, Moulatlet GM, Zuquim G, Hoorn C, Tuomisto H. 2019.** Geologically  
944 recent rearrangements in central Amazonian river network and their importance for  
945 the riverine barrier hypothesis. *Frontiers of Biogeography* **11**: 1–19.
- 946 **Sá RO, Tonini JFR, Van Huss H, Long A, Cuddy T, Forlani MC, Peloso PLV, Zaher**  
947 **H, Haddad CFB. 2019.** Multiple connections between Amazonia and Atlantic Forest  
948 shaped the phylogenetic and morphological diversity of *Chiasmocleis* Mehely, 1904  
949 (Anura: Microhylidae: Gastrophryninae). *Molecular Phylogenetics and Evolution*  
950 **130**: 198–210.
- 951 **Santos JC, Coloma LA, Summers K, Caldwell JP, Ree R, Cannatella DC. 2009.**  
952 Amazonian amphibian diversity is primarily derived from late Miocene Andean  
953 lineages. *PLoS Biology* **7**: e1000056.
- 954 **Silva SM, Peterson AT, Carneiro L, Burlamaqui TCT, Ribas CC, Sousa-Neves T,**  
955 **Miranda LS, Fernandes AM, D’Horta FM, Araújo-Silva LE, Batista R,**  
956 **Bandeira CHMM, Dantas SM, Ferreira M, Martins DM, Oliveira J, Rocha TC,**  
957 **Sardelli CH, Thom G, Rêgo PS, Santos MP, Sequeira F, Vallinoto M, Aleixo A.**  
958 **2019.** A dynamic continental moisture gradient drove Amazonian bird diversification.  
959 *Science Advances* **5**: eaat5752.

- 960 **Sheu Y, Zurano JP, Ribeiro-Júnior MA, Ávila-Pires TCS, Rodrigues MT, Colli GR,**  
961 **Werneck FP. 2020.** The combined role of dispersal and niche evolution in the  
962 diversification of Neotropical lizards. *Ecology and Evolution* **10**: 2608–2625.
- 963 **Smith BT, McCormack JE, Cuervo AM, Hickerson MJ, Aleixo A, Cadena CD, Pérez-**  
964 **Emán J, Burney CW, Xie X, Harvey MG, Faircloth BC, Glenn TC, Derryberry**  
965 **EP, Prejean J, Fields S, Brumfield RT. 2014.** The drivers of tropical speciation.  
966 *Nature* **515**: 406–409.
- 967 **Stamatakis A. 2014.** RAxML version 8: A tool for phylogenetic analysis and post-analysis  
968 of large phylogenies. *Bioinformatics* **30**: 1312–1313.
- 969 **Vacher J-P, Chave J, Ficetola F, Sommeria-Klein G, Tao S, Thébaud C, Blanc M,**  
970 **Camacho A, Cassimiro J, Colston TJ, Dewinter M, Ernst R, Gaucher P, Gomes**  
971 **JO, Jairam R., Kok PJR, Lima JD, Martinez Q, Marty C, Noonan BP, Nunes**  
972 **PMS, Ouboter P, Recoder R, Rodrigues MT, Snyder A, Marques-Souza S,**  
973 **Fouquet A. 2020.** Large scale DNA-based survey of Amazonian frogs suggest a vast  
974 underestimation of species richness and endemism. *Journal of Biogeography* **47**:  
975 1781–1791.
- 976 **Vences M, Thomas M, Bonett RM, Vieites DR. 2005a.** Deciphering amphibian diversity  
977 through DNA barcoding: chances and challenges. *Philosophical Transactions of the*  
978 *Royal Society B: Biological Sciences* **360**: 1859–1868.
- 979 **Vences M, Thomas M, van der Meijden A, Chiari Y, Vieites D. 2005b.** Comparative  
980 performance of the 16S rRNA gene in DNA barcoding of amphibians. *Frontiers in*  
981 *Zoology* **2**: 1–12.
- 982 **Wallace AR. 1854.** On the monkeys of the Amazon. *Annals and Magazine of Natural*  
983 *History* **14**: 451–454.

- 984 **Wesselingh FP, Salo JA. 2006.** Miocene perspective on the evolution of the Amazonian  
985 biota. *Scripta Geologica* **133**: 439–458.
- 986 **Wollenberg-Valero KC, Marshall JC, Bastiaans E, Caccone A, Camargo A, Morando**  
987 **M, Niemiller ML, Pabijan M, Russello MA, Sinervo B, Werneck FP, Sites Jr.**  
988 **JW, Wiens JJ, Steinfartz S. 2019.** Patterns, Mechanisms and Genetics of Speciation  
989 in Reptiles and Amphibians. *Genes* **10**: 646.

## 990 FIGURES

991



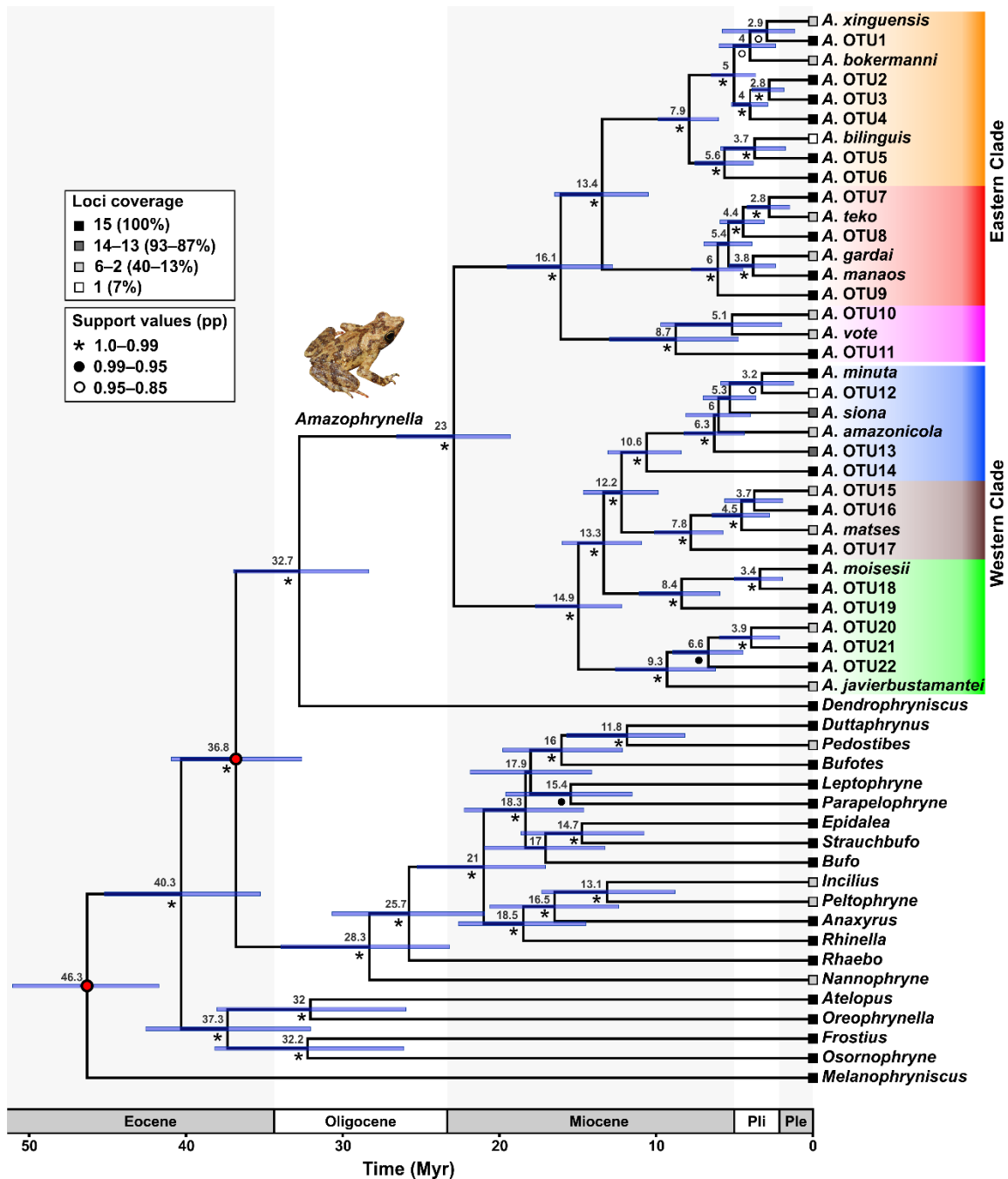
992

993 **Figure 1.** Phylogenetic relationships (A) and geographic distributions (B) of Operational994 Taxonomic Units (OTUs) inferred within *Amazophrynella*. The phylogenetic tree was

995 inferred through Bayesian optimality criteria. Nodal support values are shown close to the

996 branches (posterior probabilities below 0.8 omitted). The geographic distributions of OTUs

997 (symbols in B) are colored according to the main genetic clusters (colors in A).

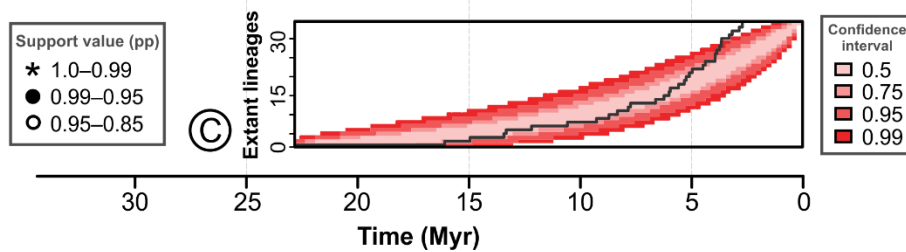
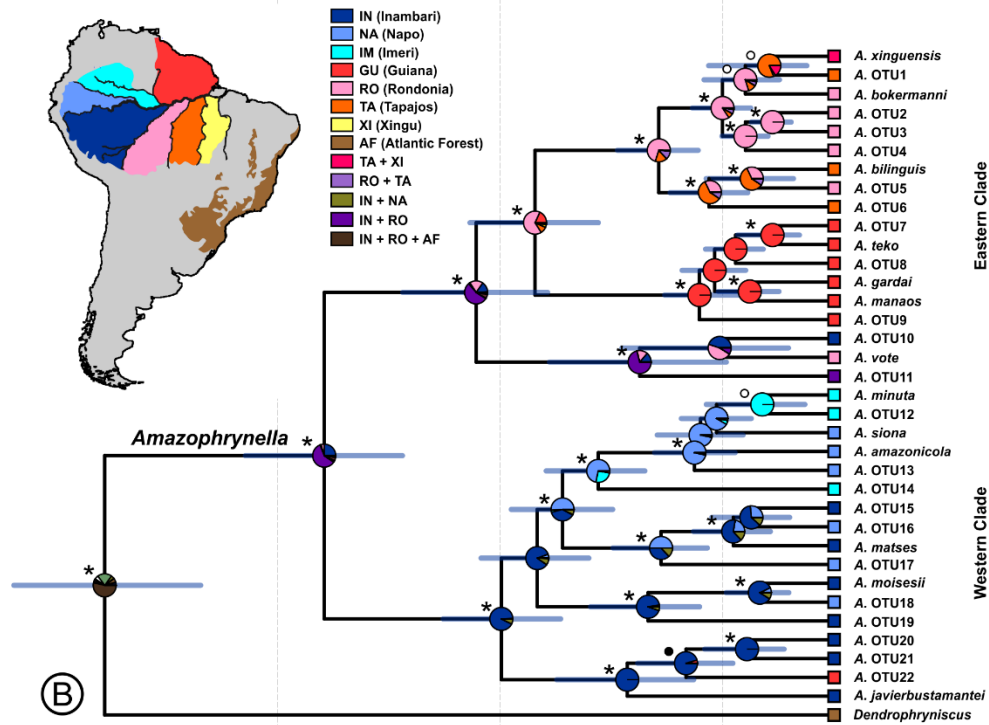
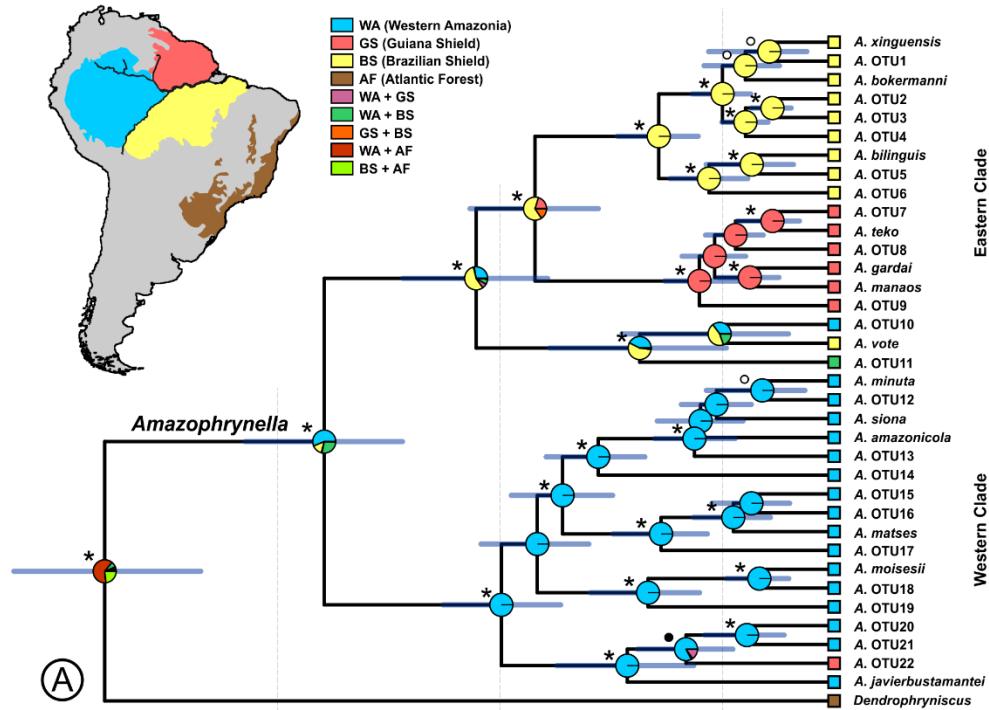


998

999 **Figure 2.** Bayesian mitogenomic time-calibrated phylogenetic tree of the family Bufonidae,  
 1000 with a focus on relationships within *Amazophrynella*. Nodal support values are shown in  
 1001 symbols below branches (posterior probabilities below 0.85 omitted), and loci coverage for  
 1002 each terminal is shown in the gray-scale squares on the tips of the tree; both are detailed in  
 1003 the inset legends. Mean value of estimated time for cladogenetic events is presented above

1004 branches, and blue horizontal bars on nodes correspond to their 95% HPD. Red dots  
1005 highlight the calibrated nodes (see Material and Methods). Colors of OTUs correspond to  
1006 those in Fig. 1. Geological epochs: (Pli) Pliocene; (Ple) Pleistocene-Holocene.





1008 **Figure 3.** Biogeographic history of the genus *Amazophrynella* inferred from  
1009 ‘BioGeoBEARS’ optimization on the mitogenomic Bayesian chronogram (Fig. 2). The  
1010 best-fit models were DIVALIKE+J for the broad spatial partitioning (Wallacean districts)  
1011 (A) and DEC+J for the refined one (Areas of Endemism) (B). Most likely ancestral areas  
1012 shown as likelihood pie charts on nodes. The current distribution of Operational Taxonomic  
1013 Units is depicted as squares at the tips of the trees, colored according to the inset legends.  
1014 The inset maps show the biogeographic areas used; for details on their riverine boundaries,  
1015 see text. Combinations of areas are considered in the respective analyses but not depicted  
1016 on the maps, and only the most likely area is presented. Nodal support values are shown as  
1017 symbols above branches, detailed in the inset legend (posterior probabilities below 0.85  
1018 omitted). Blue horizontal bars on nodes correspond to the 95% HPD of time estimates. In  
1019 (C), the temporal pattern of lineage accumulation within *Amazophrynella*, inferred with a  
1020 Lineage Through Time (LTT) plot using the same Bayesian chronogram (Fig. 2). The red  
1021 gradient in (C) indicates the confidence intervals of expected lineage accumulation under a  
1022 Yule pure-birth diversification model, and the grey line represents the empirical data.

1023 **SUPPORTING INFORMATION**

1024 **Appendix A.** DNA extraction and 16S data acquisition

1025 **Appendix B.** Mitogenome sequencing, assembling and annotation

1026 **Appendix C.** Taxonomic considerations

1027 **Table S1.** Samples included in the analyses

1028 **Table S2.** Summary of incongruences in GenBank data

1029 **Table S3.** Mean uncorrected pairwise genetic distances among OTUs

1030 **Table S4.** Summary statistics for each of the models fit to *Amazophrynella* diversification

1031 in ‘BioGeoBEARS’ analyses

1032 **Table S5.** Summary results for number and types of dispersal events during

1033 *Amazophrynella* diversification according to Biogeographical Stochastic Mapping analyses

1034 **Table S6.** Summary statistics for each of the models fit to *Amazophrynella* diversification

1035 in Lineage Through Time analyses

1036 **Figure S1.** Known distribution records of *Amazophrynella*

1037 **Figure S2.** Results of species delimitation analyses

1038 **Figure S3.** Hypothetical reconstruction of *Amazophrynella* diversification based on

1039 ancestral area reconstruction analyses and geomorphological changes in Amazonian

1040 landscape during the Neogene–Quaternary

1041 **Figure S4.** Biogeographic history of the genus *Amazophrynella* from ‘BioGeoBEARS’

1042 optimization on the mitogenomic Bayesian chronogram without considering the ‘J’

1043 parameter